Photo-microfluidic chip reactors for propene complete oxidation with TiO$_2$ photocalyst using UV-LED light

J. Fernández-Catalá, G. Garrigós-Pastor, Á. Berenguer-Murcia and D. Cazorla-Amorós*

Materials Institute and Inorganic Chemistry Department, University of Alicante, Ap. 99, E-03080 Alicante, Spain.

Corresponding author; e-mail: cazorla@ua.es

Abstract

In this study, we present a photo-microreactor illuminated with a low power LED light as a highly efficient system to achieve the total oxidation of propene using a TiO_2 photocatalyst. This abatement system (photo-microreactor) consists in an immobilized benchmark photocatalyst (TiO_2, P25) inside a commercial glass microchannel chip (UV transparent microfluidic chips, internal volume of 9.5 µL) using a packed-bed configuration without any previous treatment. The P25 inside the microreactor shows a nearly homogenous filling of the particles resulting in a low pressure drop throughout the system. In terms of propene abatement (Catalytic activity), the P25 inside the commercial microreactor reaches total propene conversion (100%) under flow conditions at low concentrations (100 ppmv) due to shorter diffusion distances, large surface-to-volume ratios, efficient heat transfer , and the improved light penetration inside the microchannel. Moreover, the prepared microreactor uses a low consumption power (LED), low residence time and presents a relatively low pressure drop making this device (P25 inside a commercial microreactor) very interesting for the abatement of volatile organic compounds at low concentration for example at indoor ambient due to its small size (45 x 15 mm).

Keywords: *Photocatalysis, VOCs, Microreactors, LEDs, TiO_2.*

1. Introduction

One of the current problems of our society is the abatement of volatile organic compounds (VOCs) when they are present at low concentrations, due to the risk they pose to human health and the environment. This type of pollutants can damage the nervous system and are strongly carcinogenic. They also present a clear connection to climate change, among other adverse effects [1-3]. VOCs are present in vehicle emissions, industrial effluents,

and also in indoor ambient. For these reasons, the scientific community is undertaking significant efforts to remove this type of pollutants [4]. The study of propene abatement is interesting because this molecule is a plausible representative example of low molecular weight VOCs and has some problems concerning the environment and human health [5-7]. The conventional removal of VOCs is by the use of catalytic combustion but this methodology needs high temperatures and pressures to reach complete oxidation [8]. On the other hand, heterogeneous Photo-Catalytic Oxidation (PCO) is very interesting to eliminate this type of pollutants since it operates under mild conditions to accomplish the abatement of VOCs [9,10]. As a rule, PCO processes use a semiconductor material as catalyst. Nowadays titanium dioxide (TiO_2) is hitherto one of the most used catalysts in photocatalysis both in gas phase and in liquid phase, due to its attractive characteristics being low production cost, nontoxicity and high photocatalytic activity the most relevant features [11,12,13] In previously reported works, usually TiO_2 is irradiated with UV light coming from conventional (xenon or mercury) lamps as energy emitters to degrade different types of VOCs. In general, these lamps exhibit low energy, nearly homogenous efficiency and poor light penetration making the complete VOCs removal an overall inefficient process [14,15]. At present, among the different types of reactors, the fixed bed reactor configuration is commonly used although this type of configuration presents a low efficiency regarding the utilization of the catalyst. One reason is attributed to the low penetration of irradiated light through the catalytic bed [16,18].

With this in mind, one solution for the total abatement of propene is the use of PhotoCatalytic Oxidation in combination with microreactor technology [17]. In the last years, the use of microreactors has aroused interest in various subjects, for example, medicine, chemistry, materials science and energy, among others [19-22]. According to reports in the literature, microreactors are used for the elimination of pollutants in

microfluidic reactors in liquid phase [23] and in organic synthesis [24] mainly due to their benefits with respect to conventional plug-flow or batch reactors. These include large surface-to-volume ratio, higher mixing efficiency, faster heat and mass transfer rates, and higher reaction rate, among others [22,25,26]. In this sense Matsushita et. al. showed that several different reactions (photocatalytic degradation , reduction, and amine N-alkylation) can be performed very rapidly with considerably large photonic efficiencies in a photocatalytic microreactor with immobilized TiO_2 layer. Moreover they observed that the photocatalytic microreactor was successful in the N-alkylation reaction in contrast to the results observed in a batch reactor. [27]. Krivec et al. presented a TiO_2-based microreactor with a highly efficient degradation of caffeine dissolved in water. This system consists of a double-layered TiO_2 anatase film immobilized on the inner walls of the photoreactor. [28] In another study by Krivec et al., a study of hydrodynamics, mass transfer, and photocatalytic activity of phenol oxidation reaction in a fixed TiO_2 microreactor was performed. The authors observed that photocatalytic phenol decomposition inside the microreactor system presented a high conversion of 79.5% with a residence time of 7.22 min. [29] Shen et al. developed glass capillaries with TiO_2 supported on the inner wall by immobilized TiO_2 nanoparticles with small particle size. This microreactor reached a total conversion of benzothiophene in 2.8 min and methyl orange in 40 s. [30] More recently Suhadolnik et al. showed that the photoelectrocatalytic degradation in microreactors is very interesting due to a strong synergistic effect between the photocatalytic and electrocatalytic processes. [31,32] The most widely reported configuration reported in the literature for the microreactor is the wall-coated configuration and the reactions are performed in liguid phase. Another interesting configuration in the microreactors is the packed-bed configuration, due to the improvement of micro-mixing performance in the catalytic bed compared to wall-coated

or other type of non-packed microchannels, moreover this configuration ensures a better contact of the reagent (liquid or gas) with the photocatalyst [33,34]. Nevertheless, this type of configuration has the immobilization of the catalyst inside the reactor as the main drawback. In this situation, the in-situ synthesis of a catalytic filling is not straightforward. Moreover, it is very important to properly control the synthesis conditions in order to generate an adequate interparticle spacing, in order to avoid high pressure drops in the system [18,20].

Concerning photochemistry, another important factor to be considered and optimized is the efficiency and homogeneity of the light irradiation upon the catalyst. In this aspect, the use of microreactors is very interesting due to their characteristically small dimensions. This property allows the use of LEDs (light emitting diodes) as lighting sources since they are significantly more power-efficient than traditional energy source as xenon or mercury lamps [35-38]. Nowadays, LEDs are replacing conventional bulb lamps because they produce light from electricity more efficiently. Moreover, LEDs can improve the intensification process carried out by photo-microreactors due to their reduced size [39].

In this work we aim at the use of a photo-microfluidic chip reactor with packed-bed configuration using TiO_2 (P25) as the active phase in order to reach the total photo-oxidation of propene (VOC), using a LED lamp to irradiate the photo-microreactor. This device represents a significant enhancement of the net photocatalytic activity (represented as CO_2 production rate) compared to the photoactivity of the same active material in a plug-flow reactor or the P25 incorporated in microcapillary reactor, previously described in the literature by our research group [18], in the abatement of propene at low concentrations in the gas phase using a low lamp output power. This photomicroreactor with P25 opens up the possibility for its use in small places (for examples indoor ambient)

5

with great propene abatement performance using a microreactor with small size, 45 x 15 mm (Figure 1).
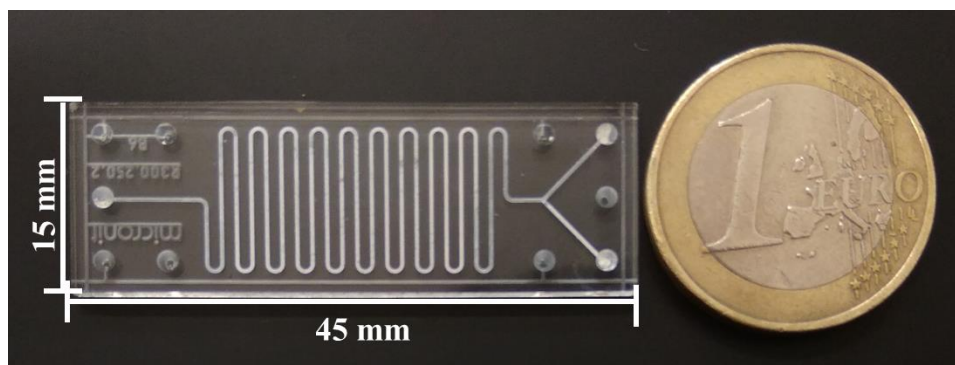

Fig. 1. Picture of the microfluidic chip reactor with a size of 45 x 15 mm used in this work and a 1€ coin with a diameter of 23 mm.

2. Materials and methods

2.1 Materials

UV light transparent microfluidic chips (Borosilicate glass) with a length of channel of 250 mm and an internal volume of 9.5 μL (Micronit Microtechnologies, Product Code: 000756) were used as microreactors. A fluidic Connect PRO Chip Holder (Micronit Microtechnologies) was used for supporting the standard 45 mm x 15 mm micro-etched glass plates to incorporate the TiO_2 and to perform the catalytic test. A LED light (LED ENGIN, model: LZ4-04UV00) with a maximum radiation peak at 365 nm and a maximum output power of 2.4 W was used to carry out the catalytic tests. A DC regulated power supply from Promax (model: FAC-662B) was used to control the output power of the LED light to perform the propene photooxidation tests.

The reagents used in this work were commercial titanium dioxide (P25, Evonik), absolute ethanol (EtOH, 99.8%, Fisher Scientific), Pluronic F-127 (F-127, Sigma-Aldrich) and deionized water. All reagents were used as received, without any further purification.

2.2 Incorporation of P25 inside the microreactor

The incorporation of a benchmark TiO_2 sample (P25) without any treatment inside the microfluidic chip was carried out by introducing a dispersion of P25 in EtOH in the presence of a surfactant (F-127). The surfactant was used with the aim of creating porosity among the P25 particles inside the microreactor, as described by our research group [18]. As an illustrative example, the incorporation of commercial P25 inside a microchannel was performed as follows: 20 mg of F-127 (15% wt. with respect to the mass of P25) were dissolved in 600 mg of EtOH (solution A). Then, 110 mg of the titanium oxide (P25) were weighed and dispersed in solution A. This dispersion was stirred vigorously for 60 min. The dispersion was injected into the microreactor (45mm x 15mm microfluidic chips, Micronit) supported in a fluidic Connect PRO Chip Holder using a 1 mL syringe. The filled microreactor was sealed and left to set at room temperature for 4h. The sealed microreactor was then annealed at 60 ºC for 24 h. After annealing, the microreactor was opened and dried overnight at 120 ºC. The filled microreactor was calcined at 350 °C for 6 h with a heating rate of 1 °C/min in order to remove the surfactant F-127 and generate the porosity among the particles of P25 inside the microreactor. This sample was labelled Microreact-P25.

2.3 Sample characterization

Optical microscopy was employed for the characterization of the commercial TiO_2 (P25) filling inside the microreactor (microscope Leica, EZ4 HD). A high sensitivity balance (Mettler Toledo, AX205 DeltaRange) with a weight resolution of 0.01 mg was used for precisely knowing the mass (mg) of P25 incorporated inside the microreactor from the difference in weight before and after filling the microreactor. It must be noted that, according to our previous work [18] the use of a surfactant and the preparation of a stable dispersion (using P25/EtOH mixtures) are two key parameters in order to successfully

and reproducibly prepare the loaded microchannels. The former is important to avoid compact photocatalyst beds which result in high pressure drops and the latter is key to obtain reproducible results.

2.4 Catalytic tests

The photocatalytic performance of the P25 incorporated in the microfluidic chips (microreactor) or in a conventional reactor, prepared for comparison purposes, was studied using two different experimental systems designed in our laboratory [18,40].

For the measurement of the catalytic activity for the abatement of propene of P25 incorporated inside the microreactor, the device was assembled in a Fluidic Connect PRO Chip Holder as shown in Figure 2. With the aim of studying the possible effect of the better illumination efficiency in the microreactor configuration, the LED light (LED ENGIN, 2.4 W, 365 nm) was connected to a DC regulated power supply (Promax, FAC-662B) to control the output power of the LED light, as shown in Table 1, using the LED manufacturer instructions. A factor to be taken into account in photocatalysis is that the irradiance (radiation power) depends on the distance from the LED to the photocatalyst as described by the Inverse-square law. In this work, the radiant flux calculated in Table 1 can be used as the irradiance in the microreactor configuration used due to the proximity between the light source and the reactor (1cm). The experimental system designed for the conventional reactor consists of a vertical quartz reactor where the photocatalyst bed (0.1g) is placed in a packed-bed configuration on quartz wool without any special immobilization protocol involved. The total reactor height is 50 mm and the catalytic bed is placed in a section of the reactor with 20 mm of diameter. This system uses a commercial UV lamp (Philips) with a power of 1 W with its radiation peak appearing at 365 nm [40]. This lamp is used for the conventional reactor and the irradiation using in this configuration is also unaffected due to the proximity between the light source and the

8

reactor (1 cm). The void volume of the photocatalyst bed in the microreactor was calculated using the bulk density of P25 and the value obtained was 96%. In the conventional reactor since the photocatalyst bed occupied a small fraction of the quartz reactor and its height could not be measured reliably, the void volume was not calculated albeit its value would be much higher than that in the microreactor.

Table 1. Voltage and intensity used in the LED light to obtain a given radiant flux (irradiance) of the LED using the manufacturer instructions.

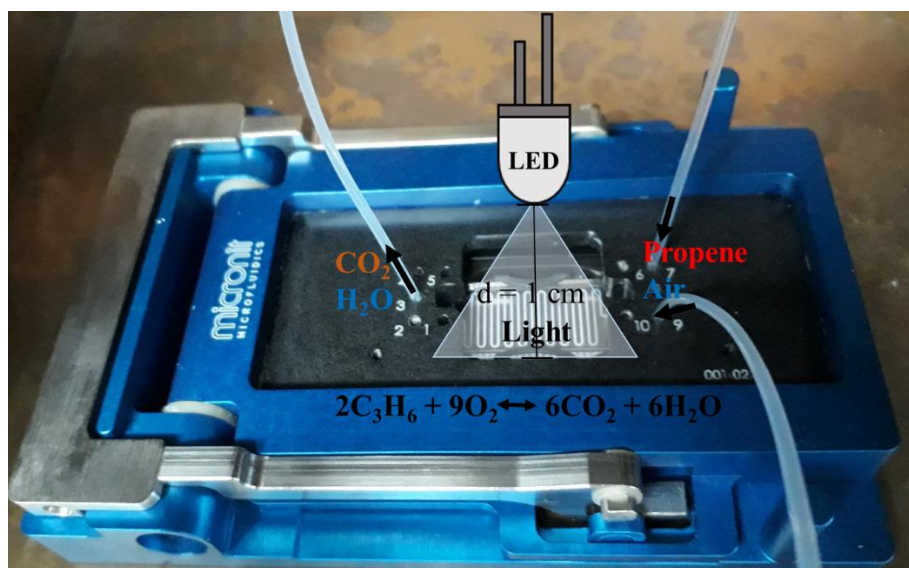| Voltage (V)	Intensity (mA)	Radiant flux (W/cm^2)
12.5	8	0.11
13	66	0.39
13.2	108	0.53
13.4	162	0.66
13.6	217	0.81
13.8	315	1.05

Fig. 2. Illustration of the experimental set up used for photocatalytic oxidation of VOCs.

The microreactor with P25 prepared in this work (Microreact-P25) was used for the total oxidation of propene at low concentrations (100 ppmv in air) at room temperature (25 ºC), as shown in equation 1. The calibrated gas cylinder was supplied by Carburos Metálicos, S.A. The propene-containing stream contained 100 ppmv of propene diluted

in synthetic air and without the addition of any humidity. The flow rate of the propene-containing stream was set at 8 (STP) ml/min and the mass of active phase (P25) inside the microreactor used in this study was 1.18 mg. In this work, we also studied the performance of the P25 in a conventional reactor using a previously reported system [40]. The flow rate of the propene-containing stream was 30 (STP) ml/min and the mass of P25 was 110 mg. Table 2 summarizes the experimental conditions used in both reactors.
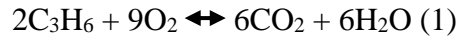
$$2C_3H_6 + 9O_2 \longleftrightarrow 6CO_2 + 6H_2O \ (1)$$

Table 2. Reactor length and volume, mass of P25 inside the microreactors and the conventional reactor, flow rate of propene, residence time used in the photooxidation experiments and registered pressure drop.

Samples	Reactor length (mm)	Reactor Volume (ml)	Mass of P25 (mg)	Propene flow (ml/min)	Residence time (mg·min/ml)	Pressure Drop (bar)
Microreact-P25	250	0.095	1.18	8	0.149	0.60
P25 in conventional reactor	50	15.7	110	30	3.66	0

The propene-containing stream was passed through the microreactor or conventional reactor with photocatalyst. The outlet was injected in a GC chromatograph (Agilent 6890N) equipped with a CTR-I column (Alltech) operating at 30 °C. GC chromatography permits to follow the evolution of the concentration of propene and CO_2 in the outlet gas. Propene conversion was calculated using the following expression (equation 2):

$$\text{Propene conversion (\%)} = \frac{C_{initial_{C_3H_6}} - C_{steady_{C_3H_6}}}{C_{initial_{C_3H_6}}} \times 100 \ (2)$$

where $C_{initial \ C_3H_6}$ is the initial propene concentration, 100 ppmv, and $C_{steady \ C_3H_6}$ is the propene concentration at steady state conditions when the UV light is switched on. Moreover, the CO_2 production rate was calculated per mol of active phase (P25) using the following expression (with the aim to normalize the results with respect to the amount active phase (P25) so as to compare both configurations):

$$CO_2 \text{ production rate } = \frac{q_{gen}}{n} \quad (3)$$

where q_{gen} is the molar flow rate of CO_2 generated (moles CO_2/s) and n is the amount in moles of catalyst (moles of P25). The mass balances were checked in all catalytic tests to corroborate that CO_2 was the only reaction product, thus corroborating the selectivity of the photocatalytic process.

Additionally, blank tests were performed under the same experimental conditions as the catalytic tests but in the absence of the TiO_2 photocatalysts. No catalytic activity was detected in any of the two reactor configurations.

3. Results and Discussion

3.1 Characterization of the active phase (P25) inside of the microreactor

The overview of the P25 filling inside the microfluidic chip (microreactor) is showed in Figure 3 a-d. Figure 3a presents an almost complete filling of the particles inside the microreactor of 300 μm in channel diameter. However, it is also possible to observe some empty spaces in the microreactor. Figures 3b-c show a good packing and immobilization of the active phase (P25) inside the microreactor observing a film of P25 on the walls of the microreactor in comparison with the empty microreactor (Figure 3d). The almost complete homogenous filling achieved and the use of the template (surfactant, Pluronic F-127), results in a low pressure drop (0.60 bar) for the microreactor with P25 (Microreact-P25) when passing the flow of propene (8 ml/min), showing that the reactor is not blocked (Table 2). This result is interesting from an applied point of view since these systems frequently suffer either of high pressure drops or complete blockage due to the compactness of the catalyst bed [18,33]. Moreover in this study we also analyzed the SEM images of P25 particles in powder form (Figure 3e,f). These SEM images show a

heterogeneous particles distribution and a high degree of interparticle space, which may favour low pressure drops throughout the reactor.
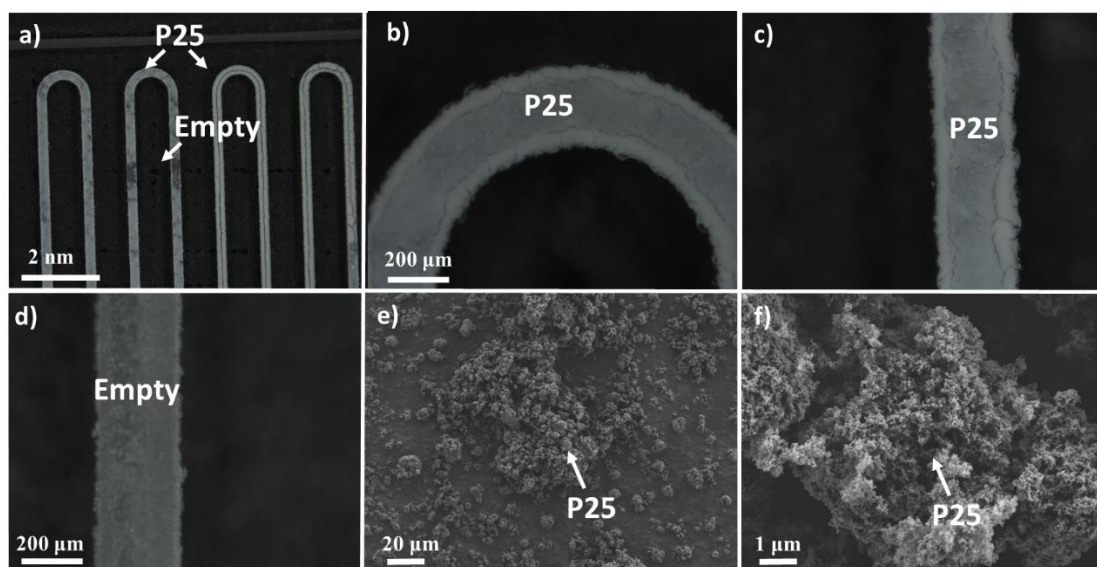

Fig 3. Microscope images of the microreactor prepared in this study: (a) Microreactor without catalyst (b, c, d) Microreactor with catalyst (Microreact-P25) at different scale. (e, f) SEM images of the P25 in powder form studied in this work at different scale.

3.2 Effect of the irradiance UV-LED upon the active phase TiO$_2$ inside a microreactor in the photocatalytic oxidation of propene.

The effect of the LED output power in the photo-microreactor (Microreact-P25) in the propene photooxidation (LED irradiance) is shown in Figure 4. The microreactor without active phase (P25) does not present any propene conversion even when setting the maximum incident radiation power on the sample at 2.4 W/cm^2. However, the sample Microreact-P25 that contained the catalytic phase (P25, 1.18 mg) showed some conversion (7%) even at low LED incident radiation power (0.1 W/cm^2). The small propene conversion under these conditions is due to the very low LED output. When the LED incident radiation power was increased, a high propene conversion was observed, reaching a total propene conversion (100%) at 0.53 W/cm^2 of LED output power. This

result is very interesting because it is indicative of the good light penetration through the catalyst with a low LED power yielding a total abatement of propene in the gas stream [16,17].
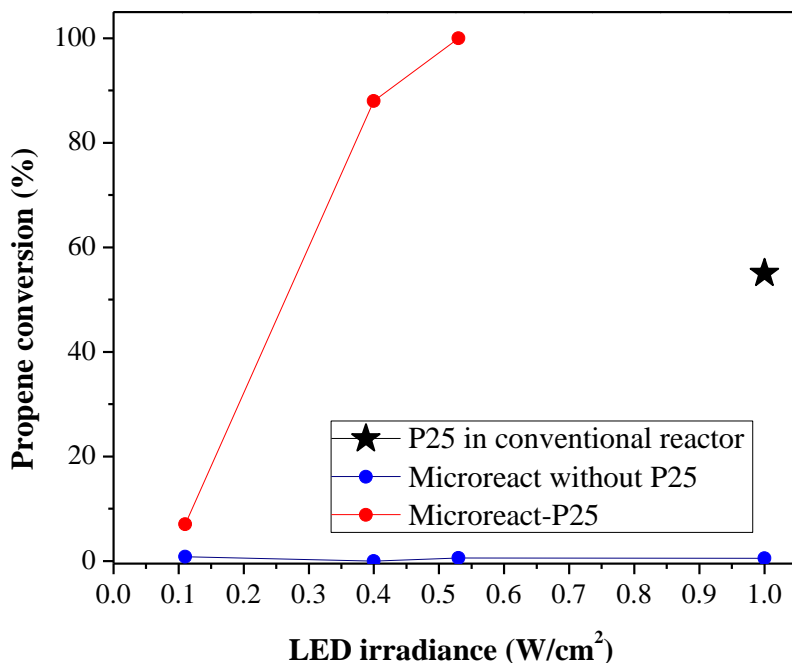

Fig 4. Photocatalytic response of the microreactor with P25 (Microreact-P25) at different UV-LED incident radiation power during the oxidation of propene at low concentration. The photocatalytic response of P25 in a conventional reactor is shown for comparison purposes. The conditions of both catalytic tests are shown in Table 2.

In addition, the effect of incident radiation power on the P25 inside the microreactor with respect to the P25 sample incorporated in a conventional reactor was compared (Figure 4 and Table 2). The Microreact-P25 presents a total propene conversion (100 %) when a flow of 8 ml/min of propene/air is passed through the sample (Microreact-P25) with a low LED power density (0.5 W/cm^2) as shown in Figure 4. However, the sample P25 incorporated in a conventional reactor presents a 60 % of the propene conversion when a stream of 30 ml/min of propene/air was passed through the conventional reactor with a

power density of 1 W/cm^2. In this sense we observed that the P25 incorporated in a microrreactor presents a higher propene conversion with respect to P25 in a convectional reactor using a low power density and a small mass of catalyst. Nevertheless the same P25 powder in a convectional reactor can use a high flow without any pressure drop as it happens in the microrreactor to a small extent. Moreover the sample Microreact-P25 present a significantly higher CO_2 production rate (moles CO_2/(s·mol P25)) with respect to the same photocatalyst in a convectional reactor. This value of CO_2 production rate is 2 orders of magnitude higher in the microreactor. This fact indicates a substantial improvement in the activity of P25 inside the microreactor due to a better illumination of the photocatalyst, an improved mixing efficiency under turbulent regime and a good contact between the catalyst and the gas due to the reduced size of the microreactor channel. In this work the amount of photocatalyst per unit of surface area of the photoreactor was also studied. The amount of P25 per unit of surface area is over one order of magnitude higher for the sample Microreact-P25 compared to the conventional reactor (0.0049 mg/mm^2 and 0.0001 mg/mm^2, respectively). This parameter indicates that a high amount of P25 in the sample Microreact-P25 is exposed on the surface of the microreactor, therefore a higher quantity of P25 is illuminated. In this work we have also obtained the quantum efficiency of the P25 incorporated in both systems for comparison purposes [41]. The sample Microreact-P25 (0.5W of power) presents a 20 % of apparent quantum efficiency (QE) and the same P25 photocatalyst in a conventional reactor (1W of power) has a QE of 16%. These values indicate that P25 inside the microreactor presents a better apparent QE with respect to the same material in a conventional reactor. However, these values are not very representative since in this study we used a UV polychromatic lamp. This light can generate misleading results as mentioned by Bolton et al in their study [42]. Moreover this result did not take into account the catalyst mass

and it was considered that all the irradiated light is absorbed by the catalyst. These considerations make the results unreliable as described by Herrmann [41].

Moreover, for comparison purposes, the catalytic properties of the P25 inside the microfluidic chips (Micronit) presented in this work, were compared with the activity catalytic of the same phase active inside a capillary (Cap.P25), previously described in the literature by our research group [18], as shown the Table 3. Sample Microreact-P25 presents a total propene conversion (100 %) and a CO_2 production rate of 0.399 moles CO_2/(s·mol P25) when a flow of 8 ml/min of propene/air is passed through the sample (Microreact-P25) with a relatively low LED power density (0.5 W/cm^2) containing only 1.1 mg of catalyst inside the microchips as shown in Table 3. These figures of catalytic activity and propene conversion are significantly higher than for sample Cap. P25. This sample (Cap. P25) presents only a 10 % of propene conversion and a CO_2 production rate of 0.069 moles CO_2/(s·mol P25), being this figure already higher than the same active phase (P25) working in a conventional reactor but much lower than for the microfluidic chip reactor. In the case of Cap. P25, a stream of 1 ml/min of propene/air was passed through the capillary reactor using a power density of 1 W/cm^2 for the LED light. In the case of the capillary, only 0.1 mg of the catalyst were placed inside the microreactor as shown in Table 3. Another important characteristic of the microfluidic chips presented in this work (Micronit) with respect to capillaries is the higher diameter (250 μm) of the channel where the active phase is incorporated with respect to capillaries (100 μm) [18]. This characteristic allows the microfluidic chips (the microreactor presented in this work) to be filled with more active phase (P25) and be able to work with larger flows than the capillaries (previously described microreactor).

Table 3. Comparison of P25 incorporated in different microreactors (microfluidic chips and capillary) and the P25 in a conventional reactor.

Samples	Mass of P25 (mg)	Propene flow (ml/min)	Residence time (mg·min/ml)	Pressure Drop (bar)	Propene conversion (%)	CO_2 production rate (moles CO_2/(s·mol P25))	Ref.
Microreact-P25	1.18	5	0.148	0.60	100	0.399	This work
P25 in conventional reactor	110	30	3.66	0	55	0.0097	This work
Cap. P25	0.1	1	0.103	0.5	10	0.069	18

These results show that sample Microreact-P25, under the conditions of analysis in this work, has a higher propene conversion and catalytic activity than the same catalyst in a convectional reactor and capillary reactor as shown Table 3. It must be remarked that the incorporation of the active phase is easy and straightforward in the case of the microfluidic chip reactor compared to the capillary probably due to its higher diameter.

In this work we have also compared our results with those obtained in the literature for commercial TiO_2 or TiO_2 synthesized in different laboratories. Nevertheless, direct comparison with previous results is difficult since the many different VOCs and analysis conditions are found in the literature. For this reason we only compare the results with works that use the same contaminant (propene) and similar conditions. In this sense it can be observed that the P25 in a microreactor as described in this work presents a better activity with respect to the same TiO_2 incorporated in a conventional reactor [43]. This fact shows the relevance of using the microreactor configuration with respect to a convectional reactor. It is also observed that the commercial TiO_2 using a film configuration [44] present a better activity with respect to P25 in a convectional reaction due to the better illumination of this configuration similar as it occurs in the microreactor configuration. However the microreactor described in this work using a packed-bed configuration presents a markedly better activity than the film configuration. In order to further improve on these results, and considering the current literature, the next step for this work will be to incorporate modified TiO_2 that can improve the activity and decrease the pressure drop.

Table 4. Overview of some similar propene photooxidation with different photocatalytic reactors performances reported in the literature.

Samples	Mass of P25 (mg)	C_i propene (ppm)	Propene flow (ml/min)	Pressure Drop (bar)	Propene conversion (%)	CO_2 production rate (moles CO_2/(s·mol cat))	Ref.
Microreact-P25 (UV-Light, 0.5 W/cm^2)	1.18	100	5	0.60	100	0.399	This work
P25 in conventional reactor (UV-Light, 1W/cm^2)	110	100	30	0	55	0.0097	This work
Hombifine N titania film (Tª 150ºC) (UV-Light)	618	300	250	0	97	0.072	[44]
TiO$_2$_Cl_Cl_20 Pack bed, Conv. React. (UV-Light, 1 W/cm^2)	110	100	60	0	58	0.019	[43]
Pd-loaded TiO$_2$ nanotubes Pack bed, Conv. React. (Vis-Light, 0.13 mW/cm^2)	25	-	2.5	0	71	-	[45]

3.3 Effect of residence time in the propene conversion in the microreactor loaded with P25

Different flows of propene with the same LED output power (1 W) were passed through the sample (Microreact-P25) maintaining the same mass of catalyst (1.18 mg) in all cases in order to study the effect of the residence time in this configuration (Table 5). Propene conversion decreases with decreasing the residence time due to a lower contact time between reagents and the catalyst surface, what is in agreement with previous studies described in the literature [37,46]. Moreover, this system was blocked (propene did not pass through sample Microreact-P25) with a propene flow over 24 ml/min due to the small diameter of the microreactor. Concerning the CO_2 production rate, this parameter increased with decreasing residence time, what can be related to the increase in pressure.

Table 5. Influence of the residence time in the microreact-P25 in terms of pressure drop, propene conversion and CO_2 production rate.

Samples	Mass of P25 (mg)	Propene flow (ml/min)	Residence time (mg·min/ml)	Pressure Drop (bar)	Propene conversion (%)	CO_2 production rate (moles CO_2/(s·mol P25))
Microreact-P25	1.18	5	0.236	0.40	100	0.249
Microreact-P25	1.18	8	0.148	0.60	100	0.399
Microreact-P25	1.18	10	0.118	0.75	99	0.498
Microreact-P25	1.18	15	0.079	1.00	77	0.560
Microreact-P25	1.18	20	0.059	1.25	61	0.589

The effect of residence time in a microreactor and a conventional reactor configurations with P25 in propene conversion are compared in Table 5. Although the residence time of the conventional reactor (3.33 (mg·min)/ml) is higher than that of the microreactor (0.148 (mg·min)/ml), the propene conversion in the microreactor configuration (microreact-P25 in Table 5) is 100% and the CO_2 production rate (moles CO_2/(s·mol P25)) is several orders of magnitude higher, which cannot be explained with the higher pressure drop of the microreactor (Table 6). The remarkable results are a consequence of the advantages of using a microreactor configuration (large surface-to-volume ratio and higher mixing efficiency, among others) and an improved illumination of the active phase (P25) [17,25]. It must be noted that concerning the mixing regime, both reactors should be comparable since both of them are made up of packed beds of small P25 nanoparticles. Under these conditions the flow of gas through the bed itself can be considered a turbulent flow regime, and thus mixing would be provided by turbulence. If the microreactor would have been prepared by wash-coating, a layer of the photocatalyst would have been deposited and thus laminar flow might be expected, but as we have shown in the manuscript (see Figure 3), the photocatalyst is deposited as a porous filling. Thus, the better performance of the sample Microreact-P25 can be attributed, among other causes, to the improved mixing efficiency in the microchannel confines.

Table 6. Comparison of the operation conditions (residence time, power density and pressure drop) and catalytic activity (propene conversion and CO_2 production rate) of both configurations (microreactor and conventional reactor).

Samples	Residence time (mg·min/ml)	Power density (W/mg·cm²)	Propene conversion (%)	CO₂ production rate (moles CO₂/(s·mol P25))	Pressure Drop (bar)
Microreact-P25	0.148	93	100	0.399	0.6
P25 in conventional reactor	3.66	3	55	0.001	0

3.5 Evaluation of the catalyst stability of the P25 incorporated in a packed-bed microfluidic chip reactor configuration

As in any heterogeneous catalytic system, cycling and stability tests are necessary to prove the interest of the catalyst from an application point of view. In the case of VOCs removal the photocatalyst can be deactivated due to the formation of physisorbed products and/or the catalyst may be removed from the reactor during operation. The catalytic activity of P25 inside of the microreactor was studied for 24 hours at two different LED output power (0.4 W and 1 W) as shown in Figure 5. The performance of the P25 inside the microreactor when irradiated with 0.4 W/cm² was partially stable for the first 6 h. Nevertheless, after 24h the propene conversion droped by 8%. In the case of the sample irradiated with an output power density of 1 W/cm² the catalyst is stable for 24 h because the irradiated light is sufficient to completely oxidize the propene that passed through the Microreact-P25 throughout the duration of stability test. Moreover, under these conditions the total propene conversion was achieved after 5 min and the temporal evolution of CO_2 concentration is stable throughout the experimental run. This is evidenced by the fact that 300 ppm of CO_2 was detected in the reactor outlet due to the total oxidation of propene once the quasi-steady state was reached.
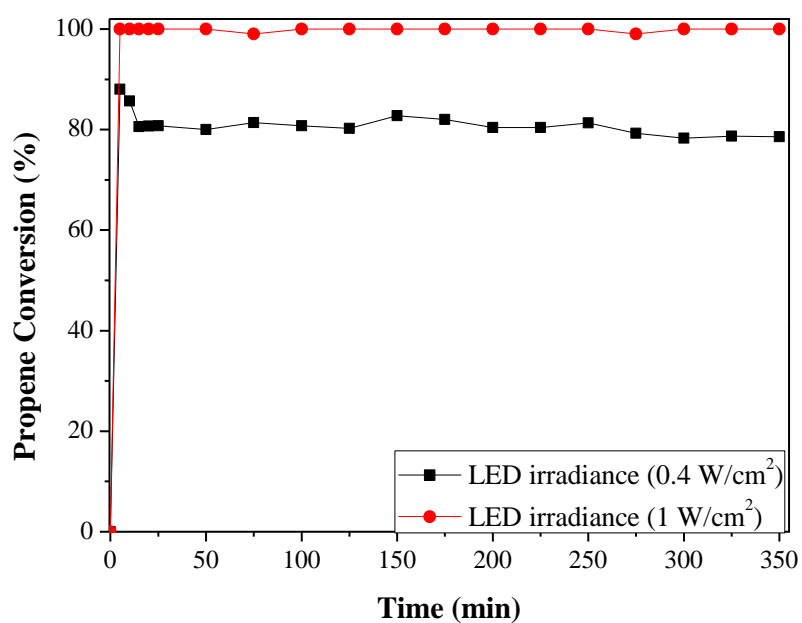
Fig. 5. Stability of the catalyst (Microreact-P25) under continuous operation at different LED output power density (0.4 W/cm^2 and 1 W/cm^2) in the total oxidation of propene.

Another test for the catalyst stability was performed by multiple consecutive on/off light cycle experiments at different light output power density (0.4 W/cm^2 and 1 W/cm^2), as shown in Figure 6. The performance of the sample did not show a noticeable change in the propene conversion value at the end of each cycle in both cases (0.4 W/cm^2 and 1 W/cm^2). Moreover, the mass balances were checked in all reactions to corroborate that CO$_2$ was the only reaction product. The mass (mg) of P25 incorporated in the microreactor did not change after the stability tests. The good results in the stability test and the high abatement capability of propene, make this Microreact-P25 system very interesting for its application in the removal of this type of contaminants in indoor atmospheres.
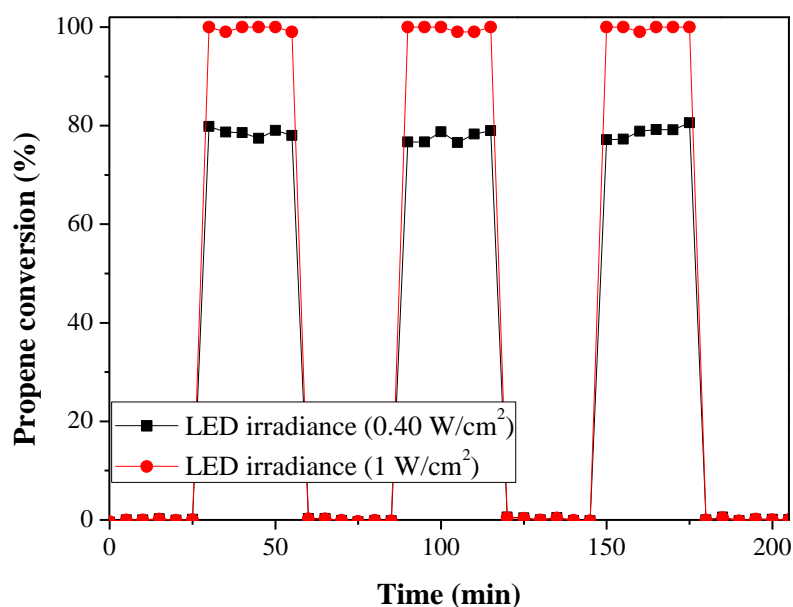
Fig. 6. Stability of the catalyst (Microreact-P25) in cyclic operation: On-Off transient experiments at different LED output power density (0.4 W/cm^2 and 1 W/cm^2) in the oxidation total of propene.

4. Conclusions

In this study, we present a photo-microfluidic chip reactor illuminated with LED which represents a highly efficient system to achieve total photocatalytic propene oxidation at low concentration, consisting on commercial TiO_2 incorporated in a commercial microreactor through a simple and straightforward experimental method. This system can totally mineralize the propene contained in air at low concentrations using a few milligrams (1.18 mg) of catalyst (TiO_2, P25) inside the microreactor using a UV-LED light (0.55 W/cm^2) and low residence time (0.14 mg·min/ml), with excellent performance in terms catalytic activity (CO_2 production rate) compared to the same catalyst in a conventional reactor and in a microcapillary reactor. Moreover, the P25 inside of the microfluidic chip reactor presents a high stability under continuous and cyclic operation

21

in the propene photooxidation under LED illumination conditions (0.4 W and 1W), which are significantly more cost-effective than conventional Hg or Xe lamps, commonly used for experiments performed under UV light. The results obtained in this work makes this system (P25 inside a microreactor) highly interesting for environmental applications in gas phase. Moreover this technology could be considered a proof-of-concept for using microreactors in environmental applications as for example the use of this system for indoor ambient purification due to its small size and high activity. Nevertheless the development of catalysts able to operate under solar/visible light irradiation would be necessary. The low amount of catalyst used in the microreactors is also an important factor since this improves the cost-efficiency of this technology, even if microchannel reactors are not cheap at present.

Acknowledgements

References

[1]   S.E. Manahan, Environmental chemistry, 8th ed., CRC Press, USA, 2004.

[2]   T. Dutta, K.H. Kim, M. Uchimiya, P. Kumar, S. Das, S.S. Bhattacharya, J. Szulejko, The micro-environmental impact of volatile organic compound emissions from large-scale assemblies of people in a confined space, Environ. Res. 151 (2016) 304–312.

[3]   I. Myers, R.L. Maynard, Polluted air - Outdoors and indoors, Occup. Med. 55 (2005) 432–438.

[4]   M. Śmiełowska, M. Marć, B. Zabiegała, Indoor air quality in public utility environments—a review, Environ. Sci. Pollut. Res. 24 (2017) 11166–11176.

[5]   Y. Lin, M. Shao, S. Lu, The emission characteristics of hydrocarbon from chinese cooking under smoke contro, Int. J. Environ. Anal. Chem. 90 (2010) 708-721.

[6] J. Fernández-Catalá, L. Cano-Casanova, M.Á. Lillo-Ródenas, Á. Berenguer-Murcia, D. Cazorla-Amorós, Synthesis of TiO_2 with hierarchical porosity for the photooxidation of propene, Molecules. 22 (2017) 2243–2259.

[7] L. Cano-Casanova, A. Amorós-Pérez, M. Ouzzine, M.Á. Lillo-Ródenas, M.C. Román-Martínez, One step hydrothermal synthesis of TiO_2 with variable HCl concentration: Detailed characterization and photocatalytic activity in propene oxidation, Appl. Catal. B Environ. 220 (2017) 645–653.

[8] R. Mével, K. Chatelain, P.A. Boettcher, G. Dayma, J.E. Shepherd, Low temperature oxidation of n-hexane in a flow reactor, Fuel. 126 (2014) 282–293.

[9] M. Kaneko, I. Okura, Photocatalysis: Science and technology, 1st ed.; Springer, Germany, 2002.

[10] L. Zhang, C. Yang, K. Lv, Y. Lu, Q. Li, X. Wu, Y. Li, X. Li,J. Fan, M. Li, SPR effect of bismuth enhanced visible photoreactivity of Bi_2WO_6 for NO abatement, Chinese Journal of Catalysis 40 (2019) 755–764.

[11] X. Chen, S.S. Mao, Titanium dioxide nanomaterials : Synthesis, properties, modifications, and applications, Chem. Rev. 107 (2007) 2891–2959.

[12] Z. Shayegan, C.S. Lee, F. Haghighat, TiO_2 photocatalyst for removal of volatile organic compounds in gas phase – A review, Chem. Eng. J. 334 (2018) 2408–2439.

[13] T. Shi, Y. Duan, K. Lv, Z. Hu, Q. Li , M. Li, X Li, Photocatalytic oxidation of acetone over high thermally stable TiO_2 nanosheets with exposed (001) facets, frontiers in Chemistry. 6 (2018) 175.

[14] C.Y Wu, Y.H. Yue, X. Deng, W. Hua, Z. Gao, Investigation on the synergetic effect between anatase and rutile nanoparticles in gas-phase photocatalytic oxidations, Catal. Today. 93 (2004) 863–869.

[15] A. Amorós-Pérez, L. Cano-Casanova, A. Castillo-Deltell, M.Á. Lillo-Ródenas, M.C. Román-Martínez, TiO_2 modification with transition metallic species (Cr, Co, Ni, and Cu) for photocatalytic abatement of acetic acid in liquid phase and propene in gas phase, Materials. 12 (2018) 40-58.

[16] C.J. Bueno-Alejo, J.L. Hueso, R. Mallada, I. Julian, J. Santamaria, High-radiance LED-driven fluidized bed photoreactor for the complete oxidation of n-hexane in air, Chem. Eng. J. 358 (2019) 1363–1370.

[17] J. Fernández-Catalá, D. Cazorla-Amorós, Á. Berenguer-Murcia, Facile encapsulation of P25 (TiO_2) in spherical silica with hierarchical porosity with enhanced photocatalytic properties for gas-phase propene oxidation, Appl. Catal. A Gen. 564 (2018) 123–132.

[18] J. Fernández-Catalá, Á. Berenguer-Murcia, D. Cazorla-Amorós, Photocatalytic oxidation of VOCs in gas phase using capillary microreactors with commercial TiO_2 (P25) fillings, Materials. 11 (2018) 1149-1159.

[19] X. Yao, Y. Zhang, L. Du, J. Liu, J. Yao, Review of the applications of microreactors, Renew. Sustain. Energy Rev. 47 (2015) 519–539.

[20]   A. Tanimu, S. Jaenicke, K. Alhooshani, Heterogeneous catalysis in continuous flow microreactors: A review of methods and applications, Chem. Eng. J. 327 (2017) 792–821.

[21]   A. Šalić, A. Tušek, B. Zelić, Application of microreactors in medicine and biomedicine, J Appl Biomed. 10 (2012) 137-153

[22]   K.S. Elvira, X.C. Solvas, R.C. Wootton, A.J. Mello, The past, present and potential for microfluidic reactor technology in chemical synthesis, Nat. Chem. 5 (2013) 905–915.

[23]   I. Azzouz, Y.G. Habba, M. Capochichi-Gnambodoe, F. Marty, J. Vial, Y. Leprince-Wang, T. Bourouina, Zinc oxide nano-enabled microfluidic reactor for water purification and its applicability to volatile organic compounds, Microsystems Nanoeng. 4 (2018) 17093.

[24]   M. Oelgemöller, O. Shvydkiv, Recent advances in microflow photochemistry, Molecules. 16 (2011) 7522–7550.

[25]   G. Kolb, V. Hessel, Micro-structured reactors for gas phase reactions, Chem. Eng. J. 98 (2004) 1–38.

[26]   T. Wirth, Microreactors in organic synthesis and catalysis, 2nd ed., Wiley-VCH, USA, 2008.

[27]   Y. Matsushita, N. Ohba, S. Kumada, K. Sakeda, T. Suzuki, T. Ichimura, Photocatalytic reactions in microreactors, Chem. Eng. J. 135 (2008) 303-308

[28]   M. Krivec, K. Žagar, L. Suhadolnik, M. Čeh, G. Drazic, Highly efficient TiO_2-based microreactor for photocatalytic applications, ACS Appl. Mater. Interfaces. 5 (2013) 9088−9094.

[29]   M. Krivec, A. Pohar, B. Likozar, G. Drazic, Hydrodynamics, mass transfer, and photocatalytic phenol selective oxidation reaction kinetics in a fixed TiO_2 microreactor, AIChE Journal. 61, (2015) 572-581.

[30]   C. Shen, Y.J. Wang, J.H. Xu, G.S. Luo, Glass capillaries with TiO_2 supported on inner wall as microchannel reactors, Chem. Eng. J. 277 (2015) 48–55.

[31]   L. Suhadolnik, A. Pohar, B. Likozar, M. Čeh, Mechanism and kinetics of phenol photocatalytic, electrocatalytic and photoelectrocatalytic degradation in a TiO_2-nanotube fixed-bed microreactor, Chem. Eng. J. 303 (2016) 292–301.

[32]   L. Suhadolnik, A. Pohar, U. Novak, B. Likozar, A. Mihelič, M. Čeh, Continuous photocatalytic, electrocatalytic and photo-electrocatalytic degradation of a reactive textile dye for wastewater-treatment processes: Batch, microreactor and scaled-up operation, J. Ind. Eng. Chem.72, (2019) 178-188.

[33]   R. Munirathinam, J. Huskens, W. Verboom, Supported catalysis in continuous-flow microreactors, Adv. Synth. Catal. 357 (2015) 1093–1123.

[34]   C. Shen, Y.J. Wang, J.H. Xu, G.S. Luo, Glass capillaries with TiO_2 supported on inner wall as microchannel reactors, Chem. Eng. J. 277 (2015) 48–55.

[35]   A. Roibu, R.B. Morthala, E.M. Leblebici, D. Koziej, T. Van Gervena, S. Kuhn, Design and characterization of visible-light LED sources for microstructured photoreactors, React. Chem. Eng. 3 (2018) 849-865.

[36]   R. Sharmin, M.B. Ray, Application of ultraviolet light-emitting diode photocatalysis to remove volatile organic compounds from indoor air, J. Air Waste Manag. Assoc. 62 (2012) 1032–1039.

[37]   F. Khodadadian, M.W. de Boer, A. Poursaeidesfahani, J.R. van Ommen, A.I. Stankiewicz, R. Lakerveld, Design, characterization and model validation of a LED-based photocatalytic reactor for gas phase applications, Chem. Eng. J. 333 (2018) 456–466.

[38]   M. Khademalrasool, M. Farbod, M.D. Talebzadeh, The improvement of photocatalytic processes: Design of a photoreactor using high-power LEDs, J. Sci. Adv. Mater. Devices. 1 (2016) 382–387.

[39]   T. Van Gerven, G. Mul, J. Moulijn, A. Stankiewicz, A review of intensification of photocatalytic processes, Chem. Eng. Process. Process Intensif. 46 (2007) 781–789.

[40]   M.Á. Lillo-Ródenas, N. Bouazza, Á. Berenguer-Murcia, J.J. Linares-Salinas, P. Soto, A. Linares-Solano, Photocatalytic oxidation of propene at low concentration, Appl. Catal. B Environ. 71 (2007) 298–309.

[41]   J. M. Herrmann, Fundamentals and misconceptions in photocatalysis, J. Photochem. Photobiol. A Chem. 216 (2010) 85-93.

[42]   J. R. Bolton, I. Mayor-Smith, K. G. Linden, Rethinking the concepts of fluence (UV Dose) and fluence rate: The importance of photon-based units - A systemic review, Photochem. Photobiol. 91 (2015)1252-1262.

[43]   M. Ouzzine, J.A. Maciá-Agulló, M.A. Lillo-Ródenas, C. Quijada, A. Linares-Solano, Synthesis of high surface area TiO_2 nanoparticles by mild acid treatment with HCl or HI for photocatalytic propene oxidation, Appl. Catal. B Environ. 154–155 (2014) 285–293.

[44]   C. T. Brigden, S. Poulston, M. V. Twigg , A. P. Walker, A. J.J. Wilkins, Photo-oxidation of short-chain hydrocarbons over titania, Appl. Catal. B Environ. 32 (2001) 63–71.

[45]   C. Li, L. Zong, Q. Li1, J. Zhang, J. Yang, Z. Jin, Photocatalytic oxidation of propylene on Pd-Loaded Anatase TiO_2 nanotubes under visible light irradiation, Nanoscale Research Letters. 11 (2016) 271.

[46]   J. Jeong, K. Sekiguchi, W. Lee, K. Sakamoto, Photodegradation of gaseous volatile organic compounds (VOCs) using TiO_2 photoirradiated by an ozone-producing UV lamp: decomposition characteristics, identification of by-products and water-soluble organic intermediates, J. Photochem. Photobiol. A Chem. 169 (2005) 279–287.